

B.T. Wolschrijn, D. Voigt, R. Jansen, R.A. Cornelussen, N. Bhattacharya, R.J.C. Spreeuw and H.B. van Linden van den Heuvell

*Van der Waals-Zeeman Institute, University of Amsterdam,  
Valckenierstraat 65, 1018 XE Amsterdam, the Netherlands  
e-mail: spreeuw@wins.uva.nl*

(February 1, 2001)

We report direct observation of a rainbow caustic in the velocity distribution of  $^{87}\text{Rb}$  atoms, bouncing inelastically on an evanescent-wave atom mirror. In contrast to known examples, this caustic is caused by a stochastic process, namely a spontaneous Raman transition during the bounce. The results are in good agreement with a classical calculation. We observed that although energy is extracted from the atoms, the phase-space density is in most cases not increased.

32.80.Lg, 42.50.Vk, 03.75.-b

Caustics are ubiquitous phenomena in nature. Examples are the cusp-shaped patterns of light reflection on the inside of a coffee-cup and the patterns of bright lines observed on the bottom of a swimming pool [1]. The prime example of a caustic is the common rainbow, which can be understood in a ray-optics picture by considering how the scattering angle of a light ray depends on its impact parameter on a water droplet [2]. Whereas the incident rays have smoothly distributed impact parameters, the outgoing rays pile up where the scattering angle has a local extremum. Such a divergence of the ray density, the caustic, appears at the rainbow angle. In atomic [3] and nuclear [4] scattering experiments analogous rainbow phenomena have also been observed.

The examples of caustics that have been known so far have in common that the outgoing parameter (scattering angle) is a *deterministic* function of the incoming parameter (impact parameter). In this Letter we report on our observation of a new type of rainbow caustic existing by virtue of a *stochastic* process, which distributes a single-valued “impact parameter” over a range of “scattering angles”. To our knowledge, this type of caustic has not been observed before.

We have observed this caustic in the velocity distribution of cold atoms, after bouncing inelastically off an evanescent-wave mirror [5–7]. The incident atoms are monochromatic, i.e. they all have the same velocity. During the bounce the atoms are optically pumped to a different hyperfine ground-state, by a spontaneous Raman transition. They leave the surface with less kinetic energy, due to the difference in optical potential. Our measurements and analysis show that the resulting velocity distribution is highly asymmetric, containing a caustic at the minimum velocity. This divergence demonstrates the strong preference for making the Raman transition in the

turning point.

We briefly discuss the divergence in the velocity distribution in the context of evanescent-wave cooling [5,7]. Calculations show that although energy is extracted from the atoms, a single inelastic bounce generally leads to a decrease of phase space density.

The experiment is performed in a rubidium vapor cell. We trap about  $10^7$  atoms of  $^{87}\text{Rb}$  in a magneto-optical trap (MOT) and subsequently cool them in optical molasses to 15  $\mu\text{K}$ . The MOT has a  $1/e^2$  radius of 0.6 mm and is centered 5.8 mm above the horizontal surface of a right-angle BK7 prism. At this surface, we create an evanescent wave (EW) by a Gaussian shaped laser beam of 0.8 mm  $1/e^2$  radius, which undergoes total internal reflection.

When blue detuned, the EW induces a repulsive optical dipole potential  $U_F(z) = U_F(0) \exp(-2\kappa z)$ , where the subscript  $F = 1, 2$  denotes the hyperfine ground state,  $\kappa = k_0 \sqrt{n^2 \sin^2 \theta - 1}$ , with  $k_0 = 2\pi/\lambda$  the free space wave vector of the light,  $n = 1.51$  the refractive index and  $\theta$  the angle of incidence [8–10]. The maximum potential  $U_F(0) \propto I_0/\delta_F$ , where  $I_0$  is the incident intensity at the glass surface, and  $\delta_F$  is the detuning. Here we define the detuning  $\delta_{1,2}$  relative to the transition  $5S_{1/2}(F = 1, 2) \rightarrow 5P_{3/2}(F' = F + 1)$  of the  $D_2$  line (780 nm), see Fig.1.

An atom entering the EW in the  $F = 1$  state is slowed down by the potential  $U_1(z)$ . Spontaneous Raman-scattering can transfer the atom to the higher hyperfine ground state ( $F = 2$ ). When transferred into this state, the potential acting on the atom is  $U_2(z)$ , which is weaker due to the increase of the detuning by approximately the hyperfine splitting  $\delta_2 \approx \delta_1 + \delta_{\text{hfs}}$  (Fig.1). The ratio of the two potentials,  $\beta \equiv U_2(0)/U_1(0)$ , quantifies the reduction in potential energy. As a result the atoms will bounce inelastically, i.e. to a lower height than their initial release position.

Experimental data of bouncing atoms are taken by absorption imaging. After a variable time delay the atomic cloud is exposed to 20  $\mu\text{s}$  of probe light, resonant with the  $5S_{1/2}(F = 2) \rightarrow 5P_{3/2}(F' = 3)$  transition. Thus only atoms which have been transferred to  $F = 2$  contribute to the signal. The atomic cloud is imaged on a digital frame-transfer CCD camera. The presented images show an area of  $2.2 \times 4.5 \text{ mm}^2$  with a pixel resolution of 15  $\mu\text{m}$  (Fig.2). The initial position of the MOT is outside the field of view. The horizontal line at the bottom shows

the prism surface.

A typical series with 2 ms time increments is shown in Fig.2. Each density profile has been converted in a horizontal line sum. The solid curve is the result of a calculation described below. The amplitude of the experimental curves is rescaled such that the maximum optical density of the experimental curve coincides with the theoretical maximum value. This is the only fit parameter.

As expected, the atoms bounce up less high than their initial height. Furthermore, the spatial distribution shows another striking feature: it displays a high density peak at low  $z$ , and a long low-density tail extending upward. Note also that there is a time-focus: the density peak is sharpest when the slowest atoms reach their upper turning point. This density peak is an immediate consequence of a caustic appearing at the minimum possible velocity.

The caustic can be understood by considering the atoms as point particles moving in the EW potential. This corresponds to the ray-optics limit for the optical rainbow. We consider an atom arriving at the surface in its  $F = 1$  hyperfine ground state, with an initial downward velocity  $v_i < 0$ . Its trajectory through phase space is determined by energy conservation:  $U_1(0) \exp(-2\kappa z) + \frac{1}{2}mv_i^2 = \frac{1}{2}mv_f^2$ , and is depicted in Fig.4 by the thick line. While it is slowed down by the EW it may scatter a photon at a velocity  $v_p$ , and be transferred to the  $F = 2$  state. The atom continues on a new trajectory determined by  $U_2(z)$ . To illustrate the formation of the caustic, possible trajectories starting at various positions in phase space are depicted as thin black ( $v_p < 0$ ) and gray ( $v_p > 0$ ) curves. For asymptotically large  $z$  the density of curves represents the outgoing velocity distribution, showing the caustic where the trajectories pile up. This distribution is similar to a rainbow. The density of outgoing trajectories diverges at the "rainbow velocity". Below this velocity the intensity is zero, similar to Alexander's dark band in the optical rainbow. Above the rainbow velocity the intensity distribution decreases smoothly.

Despite the similarities, there is a crucial difference between a rainbow created by sunlight refracted by water droplets and our 'velocity caustic'. The appearance of a rainbow is usually a *deterministic* process, where the scattering angle is uniquely determined by the impact parameter. In our experiment the incoming velocity  $v_i$  is single-valued, and is distributed over a range of outgoing velocities by the *stochastic* process of spontaneous Raman scattering.

The position of our caustic is independent of  $\kappa$ , like in the optical rainbow, where the rainbow angle does not depend on the droplet size. To check this, we measured for three different values of the decay length  $\kappa^{-1}$  the atomic density profile at the upper turning point (Fig.3c). This is defined as the highest position reached by the peak density. The shape of the cloud did not change, but the number of atoms decreased with decreasing  $\kappa$  since the total number of scattered photons is lower.

By varying the detuning,  $\beta$  is changed, resulting in a

change of the rainbow velocity. Note that this amounts to varying the "degree of dissipation." This is analogous to the dependence of the rainbow angle on the refractive index. For various values of the detuning we measured the upper turning point, as a fraction of the initial MOT height (Fig.4a,b).

In order to quantitatively analyze our experimental data, we write the optical hyperfine-pumping rate during the bounce as  $\Gamma'(z) = (1 - q)\Gamma U_1(z)/\hbar\delta_1$ , where  $q$  is the branching ratio to  $F = 1$ . We define  $\eta(v)$  as the survival probability for the atom to reach the velocity  $v$  without undergoing optical pumping. This function decreases monotonically as  $\dot{\eta} = -\Gamma'\eta$ , with  $\eta(v_i) = 1$ . For  $|v| \leq |v_i|$ , the solution is  $\eta(v) = \exp(-(v - |v_i|)/v_c)$ , where  $v_c \equiv 2\kappa\hbar\delta_1/(1 - q)m\Gamma$ , with  $m$  the atomic mass. When the pumping process takes place at a certain velocity  $v = v_p$ , the atom leaves the surface with velocity  $v_f = \sqrt{v_p^2(1 - \beta) + \beta v_i^2}$  (Fig.1). This results in a distribution of bouncing velocities, resulting from atoms which were pumped while moving toward ( $v_p^-$ ) or away from ( $v_p^+$ ) the surface:  $n(v_f) = \eta(v_p^-(v_f)) \times |\frac{\partial v_p^-}{\partial v_f}| + \eta(v_p^+(v_f)) \times |\frac{\partial v_p^+}{\partial v_f}|$  for  $\sqrt{\beta}|v_i| \leq v_f < |v_i|$ , which diverges at  $v_f = \sqrt{\beta}|v_i|$ . This velocity caustic originates from atoms which are pumped near the turning point. There are two reasons for scattering preferentially at this position. An atom spends a relatively long time in the turning point since its velocity is lowest there. In addition, the intensity of the EW, and thus the photon scattering rate is highest in the turning point. The divergence is an artefact of the ray-optics description. It disappears due to diffraction when the atoms are treated as matter waves.

To compare the experimentally obtained spatial distributions with the model, we first calculated the one-dimensional phase-space density  $\rho(z, v)$ . The spatial distribution is obtained by projecting  $\rho$  on the  $z$ -axis. Initially the MOT is described by a normalized gaussian,  $\rho(z, v) \propto \exp(-(z - z_0)^2/2\sigma_z^2) \exp(-v^2/2\sigma_v^2)$  with  $z_0 = 5.8$  mm,  $\sigma_z = 0.3$  mm and  $\sigma_v = 3.8$  cm/s. This distribution falls due to gravity and expands due to thermal motion. When it arrives at the EW it is reflected, and the velocity distribution is changed in the way described above. We measure the spatial distribution of inelastically bounced atoms after a time of flight  $t$ . To illustrate the agreement with the experimental data, the result for a time  $t = 7$  ms is drawn as the thick line in Fig.2.

Considering the divergence in the distribution of outgoing velocities, it is interesting to calculate the maximum phase space density  $\rho_{max}$ , in the context of evanescent-wave cooling. Due to the broad outgoing velocity distribution, an unexpected result followed: although energy is removed from the atoms, the pumping process leads to a decrease of the maximum value of the phase-space distribution. After the bounce,  $\rho_{max}$  is roughly five times lower than the initial  $10^5$  sm $^{-2}$  per atom of the MOT for our experimental conditions. Note that this is a one-dimensional calculation; trans-

verse spreading is ignored.

When we compare  $\rho_{max}$  of the bounced atoms with that of MOT:  $\rho_{max} = \alpha \times \rho_{MOT}$ , we find that the condition for  $\alpha > 1$  is mainly determined by  $\beta$  and  $v_c$  (both depending on the detuning), and the falling height  $h$ . Note that the increase of  $\rho_{max}$  does not violate Liouville's theorem. This is possible due to the spontaneous character of the Raman transition. In Fig. 5,  $\alpha$  is plotted as a function of  $\delta_1$  and  $h$ . For a fixed falling height,  $\alpha$  reaches a maximum for a detuning  $\delta_1$  such that  $2v_c = |v_i|$ . This condition corresponds to a maximum pumping rate,  $\eta(0)\Gamma'$  in the turning point. In the limit of low  $v_c$ , the scattering rate at the turning point is low. When  $v_c$  is too high the  $F = 1$  state is too quickly depleted which also results in a low scattering rate. Decreasing the fall height also yields a higher  $\alpha$  since this determines the velocity of the atoms arriving at the EW, hence the duration of the bounce. This means that in EW-cooling experiments, the first bounces reduce the falling height but lead to a decrease of  $\rho_{max}$ . Only during later bounces can  $\rho_{max}$  increase, i.e. can the cloud be cooled. It should be noted that this calculation is only valid for a single inelastic bounce with an initial narrow distribution. After many bounces the distribution will become barometric [11].

A very intriguing aspect of our experiment is the possibility to observe supernumeraries: interference of two trajectories with the same outgoing velocity, but with different pumping velocity  $v_p$ . In the velocity distribution after the inelastic bounce, the high velocity tail is the sum of two contributions: from atoms which move towards and atoms moving away from the surface when they are pumped to  $F = 2$ . Interference between these two paths should result in oscillations in the velocity distribution. This is a nontrivial effect because it involves the spontaneous emission of a photon.

Given our experimental parameters, we expect a typical oscillation period of 1 cm/s. This spacing depends on  $\kappa$ , just as in a rainbow the supernumeraries depend on the droplet size. These oscillations are not yet resolved in our measurements, because in the EW-field the magnetic substates are not degenerate, each producing a different velocity distribution.

In conclusion, we observed a new type of caustic due to the *stochastic* distribution of a monochromatic input. This distribution is similar to the common rainbow. The caustic appears in the velocity distribution of inelastically bouncing rubidium atoms on an optical evanescent-wave atom mirror. Calculations describing the phase space evolution of the atomic cloud show that an increase as well as a decrease of the phase-space density is possible.

This work is part of the research program of the "Stichting voor Fundamenteel Onderzoek van de Materie" (FOM) which is financially supported by the "Nederlandse Organisatie voor Wetenschappelijk Onderzoek" (NWO). R.S. has been financially supported by the Royal Netherlands Academy of Arts and Sciences.

- [1] M.V. Berry, in Les Houches, Session XXXV (1980), *Physics of defects*, R. Balian *et al.*, eds., (North Holland, 1981) p. 455-543.
- [2] H.M. Nussenzveig, Sc. Am. **236**, (1977).
- [3] K.W. Ford and J.A. Wheeler, Ann. Phys. **7**, 287 (1959); D. Beck J. Chem. Phys. **37**, 2884 (1962).
- [4] M.E. Brandan and G.R. Satchler, Phys. Rep. **285**, 143 (1997).
- [5] J. Söding, R. Grimm and Yu.B. Ovchinnikov, Opt. Comm. **119**, 652 (1995)
- [6] P. Desbiolles, M. Arndt, P. Szriftgiser, and J. Dalibard, Phys. Rev. A **54**, 4292 (1996);
- [7] D.V. Laryushin, Yu.B. Ovchinnikov, V.I. Balykin, and V.S. Letokhov, Opt. Comm **135**, 138 (1997);
- [8] R.J. Cook and R.K. Hill, Opt. Comm. **43**, 258 (1982).
- [9] V.I. Balykin, V.S. Letokhov, Yu.B. Ovchinnikov, and A.I. Sidorov, JETP Lett. **45**, 353 (1987)
- [10] D. Voigt, B.T. Wolschrijn, R. Jansen, N. Bhattacharya, R.J.C. Spreeuw, and H.B. van Linden van den Heuvell, Phys. Rev. A **61**, 063412 (2000)
- [11] Yu.B. Ovchinnikov, I. Manek, and R. Grimm, Phys. Rev. Lett. **79**, 2225 (1997)

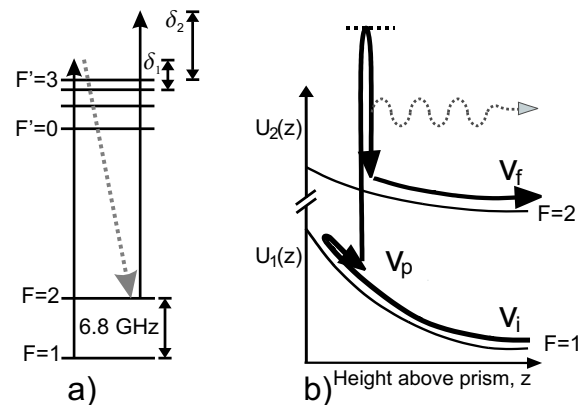


FIG. 1. (a) Involved atomic levels of  $^{87}\text{Rb}$  (b) An atom enters the evanescent wave in its  $F = 1$  state with initial velocity  $v_i$ . It is decelerated and spontaneously scatters a photon at a velocity  $v_p$ . After being pumped to  $F = 2$  it accelerates and leaves the potential with asymptotic velocity  $v_f$ .

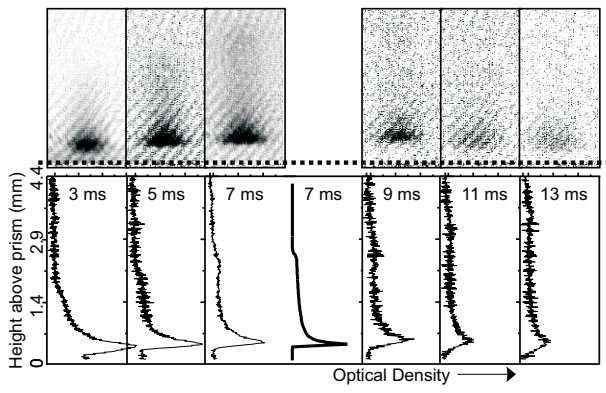


FIG. 2. Absorption images ( $2.2 \times 4.5 \text{ mm}^2$ ) at different moments after bouncing on an EW, with detuning  $92\Gamma$ , and  $\kappa^{-1} = 1 \mu\text{m}$ . A line sum shows the atomic density distribution above the prism. The dotted line indicates the prism surface. The initial MOT was located at 5.8 mm above the surface. The thick curve in the middle is the result of our calculation at 7 ms.

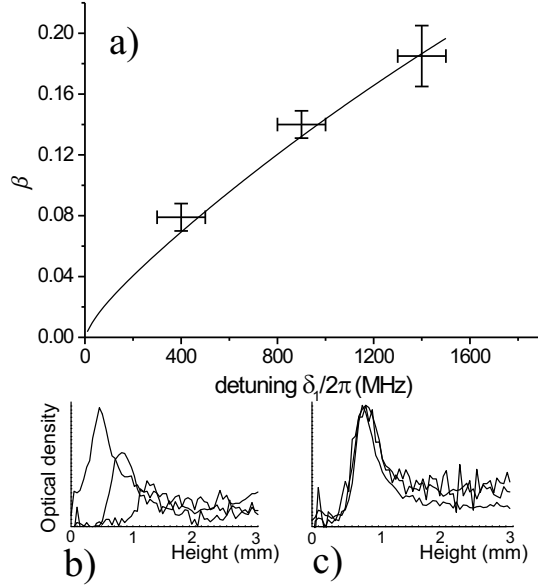


FIG. 3. a) Measured height of the upper turning point as a fraction of the initial (MOT) height. This represents  $\beta$ , the relative optical potential strength of the  $F = 1$  and  $F = 2$  ground states. The curve results from a calculation including the full level structure. b) Density profiles for various detunings:  $\delta_{EW} = 67, 150$  and  $233\Gamma$ . The curves are measured at the moment that the density peak reaches its highest point and have the same scale. c) Density profiles at  $t = 14$  ms after the bounce for  $\kappa = 1.96 \mu\text{m}$ ,  $0.80 \mu\text{m}$  and  $0.62 \mu\text{m}$ ,  $\delta_{EW} = 150\Gamma$ . The results are rescaled such that the density peaks are equally high. Variation of  $\kappa$  in this range, has no influence on the position and shape of the spatial density profile.

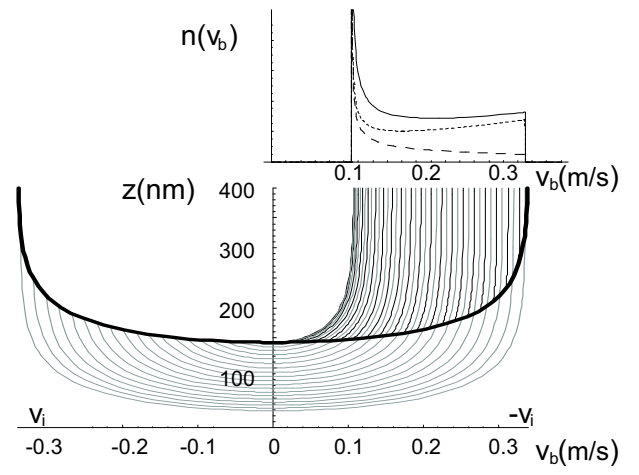


FIG. 4. Construction of the velocity caustic in terms of phase space trajectories. The velocity of the incident atoms is  $v_i = -0.34$  m/s. The thick solid line shows the trajectory of the lower hyperfine state bouncing elastically. If the atom is pumped to the other hyperfine state it continues on a different trajectory. The thin lines represent possible outgoing paths, each starting at a different pumping velocity, depending on the position of Raman-transfer. The density of outgoing trajectories diverges, yielding a caustic in the velocity distribution. Shown in the upper curve are the total distribution (solid line), and the contribution of atoms moving towards (dashed) and away from (dotted) the surface while being transferred.

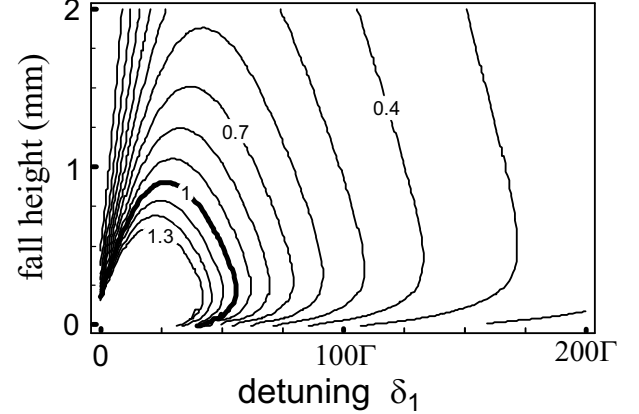


FIG. 5. Contourplot of the ratio ( $\alpha$ ) of phase space density after and before the inelastic bounce. The thick line corresponds to  $\alpha = 1$ . Other parameters were fixed:  $\kappa = 1.3 \times 10^6 \text{ m}^{-1}$ , MOT radius  $0.3 \text{ mm}$ ,  $T = 15 \mu\text{K}$ .